JOURNAL OF MATERIALS SCIENCE 4 (1969) 152–165

Anisotropy in Oriented Fibres from Synthetic Polymers

D. W. HADLEY
J. J. Thomson Physical Laboratory, The University, Reading, UK

P. R. PINNOCK
Imperial Chemical Industries Fibres Limited, Harrogate, Yorks, UK

I. M. WARD
H. H. Wills Physics Laboratory, The University, Bristol, UK and Imperial Chemical Industries Limited, Petrochemical and Polymer Laboratory, Runcorn, Cheshire, UK

Received 9 September 1968

On the assumption that synthetic fibres at low strains can be considered as transversely isotropic *elastic* bodies the five independent elastic compliances have been measured for filaments of low and high density polyethylene, nylon 6.6, polyethylene terephthalate and polypropylene, all at room temperature. Experimental values are compared with those predicted using an aggregate theory which assumes that the partially oriented fibre can be considered as an aggregate of elastic units which are aligned by the drawing process, and whose properties are those of the fully oriented fibre.

The applicability of this aggregate theory is discussed, and possible explanations are advanced in those cases where agreement between theory and experiment is unsatisfactory.

1. Introduction

Useful fibres from synthetic polymers show a characteristic anisotropy, resulting from their production by uniaxial stretching processes. There is a high degree of molecular alignment along the fibre axis giving transverse isotropy in a plane perpendicular to this axis. All the fibres discussed in this report behave as viscoelastic solids; if, however, measurements are made at a fixed time after the application of load, the effects of creep and stress relaxation can be neglected and the fibres to a first approximation regarded as anisotropic *elastic* solids. The discussion will be confined to cases where such an approximation may be justified.

At small strains the mechanical behaviour can be defined, as outlined below, in terms of five independent elastic compliances (or stiffnesses).

Recent developments have enabled all five elastic constants to be measured and results have already been reported for two selected monofilaments of polyethylene terephthalate and one monofilament of nylon 6.6. Data on extensional and shear moduli of polyethylene terephthalate and polypropylene fibres have also been published previously. Reviews of this earlier work have been made by Ward [1] and Ward and Pinnock [2]. The present paper reports a systematic attempt to measure all five elastic constants on fibre monofilaments of five materials (polyethylene terephthalate, nylon, polypropylene, low density polyethylene and high density polyethylene) at room temperature as a function of molecular orientation as determined by stretch- (or draw-) ratio.

All the results presented for low density and high density polyethylene fibres have not been reported previously. The results for the other fibres are much more extensive than those reported previously, particularly in nylon where only the single monofilament was measured.

There is some overlap with previous published work in oriented sheets of low density polyethylene and polyethylene terephthalate. Such

investigations yield two of the elastic constants explicitly and a combination of two more. (See [2] for a summary, also sections 4 and 5 below.)

Attempts have been made previously to predict the optical and mechanical anisotropy of polyethylene terephthalate and polypropylene fibres, and polyethylene fibres and films on the basis of a theory in which the fibre or film is assumed to consist of an aggregate of small anisotropic units.These attempts were incomplete because not all the elastic constants were determined. The results presented in this paper now enable such calculations to be carried out in some detail, and also provide accessible data for testing alternative theories of orientation.

2. Theoretical Principles

2.1. Anisotropic Elastic Behaviour

The mechanical properties of an anisotropic solid for small strains, are defined by the generalised Hooke's law.

$$e_p = S_{pq}\,\sigma_q$$
$$\sigma_q = C_{qp}\,e_p$$

relating strains e_p to stresses σ_q, where S_{pq} and C_{qp} are the compliance and stiffness constants respectively, p and q have integral values in the range 1 . . . . 6. (See, for example, Hearmon 1956 [3].) Transverse isotropy reduces the number of independent elastic constants to five and the matrix relation between strain and stress may then be written as (see, for example, Nye 1957 [4]).

$$e_p = \begin{matrix} S_{11} & S_{12} & S_{13} & 0 & 0 & 0 \\ S_{12} & S_{11} & S_{13} & 0 & 0 & 0 \\ S_{13} & S_{13} & S_{33} & 0 & 0 & 0 \\ 0 & 0 & 0 & S_{44} & 0 & 0 \\ 0 & 0 & 0 & 0 & S_{44} & 0 \\ 0 & 0 & 0 & 0 & 0 & 2(S_{11}-S_{12}) \end{matrix} \sigma_q \quad .$$

Compliance constants have been used rather than stiffness constants because they are more readily determined by direct experiment. These constants are simply related to the better known moduli and Poisson's ratios. (i) S_{33} is the reciprocal of Young's modulus, the extensional modulus E_0; (ii) S_{11} is the reciprocal of the transverse modulus E_{90}, perpendicular to the axis of drawing; (iii) the Poisson's ratios associated with longitudinal extension, $\nu_E = -S_{13}/S_{33}$; (iv) in a similar manner Poisson's ratios for application of a load in a plane perpendicular to a fibre axis are given by $\nu_T = -S_{12}/S_{11}$, $\nu_T' = S_{13}/S_{11}$; (v) S_{44} is the reciprocal of the torsional modulus G.

2.2. The Aggregate Theory

The aggregate theory for optical and mechanical anisotropy in polymers has been described in detail elsewhere [5], and here only its main features will be summarised.

A partially oriented fibre is assumed to consist of an aggregate of anisotropic units, each possessing transverse isotropy. The polarisability of a unit is defined by P_1 the principal polarisability of the unit parallel to its symmetry axis and P_2 the polarisability in a plane perpendicular to this axis. Let the axis of a given unit make an angle θ with the fibre axis. The birefringence for an intermediate degree of molecular orientation can then be derived as $\Delta n = \Delta n_{max}(1 - \frac{3}{2}\overline{\sin^2\theta})$, where Δn_{max} is the maximum birefringence for a completely oriented fibre and $\overline{\sin^2\theta}$ is the mean value of $\sin^2\theta$ for the aggregate.

When the calculation is extended to predict mechanical anisotropy the transformation formulae become lengthy, because the quantities involved are fourth rank tensors. The calculations can, in principle, be made in two ways, either by considering compliances or stiffnesses. In general the principal axes of stress and strain in an anisotropic solid are not coincident, and both approaches involve an approximation. One may assume either uniform stress, in which case the strains throughout the aggregate are not continuous, or uniform strain, which gives rise to discontinuity of stress. The uniform stress approach implies a summation of compliance constants, and gives rise to what will be termed the Reuss average [6]; the uniform strain method, implying a summation of stiffness, leads to the Voigt average [7].

Compliances for the aggregate are given by:

$$\bar{S}'_{33} = \overline{\sin^4\theta}\,S_{11} + \overline{\cos^4\theta}\,S_{33} + \overline{\sin^2\theta\cos^2\theta}\,(2S_{13} + S_{44})$$

$$\bar{S}'_{44} = \overline{(2\sin^2\theta\cos^2\theta + \sin^2\theta)}\,S_{11} - \overline{\sin^2\theta}\,S_{12} - \overline{4\sin^2\theta\cos^2\theta}\,S_{13} + \overline{2\sin^2\theta\cos^2\theta}\,S_{33} + \tfrac{1}{2}\overline{(\cos^4\theta + \sin^4\theta - 2\sin^2\theta\cos^2\theta + \cos^2\theta)}\,S_{44}$$

$$\bar{S}'_{11} = \tfrac{1}{8}\overline{(\cos^4\theta + 2\cos^2\theta + 3)}\,S_{11} + \tfrac{1}{4}\overline{(3\cos^2\theta\sin^2\theta + \sin^2\theta)}\,S_{13} + \tfrac{3}{8}\overline{\sin^4\theta}\,S_{33} + \tfrac{1}{8}\overline{(3\sin^2\theta\cos^2\theta + \sin^2\theta)}\,S_{44}$$

$$\bar{S}'_{12} = \tfrac{1}{8}\overline{(\cos^4\theta - 2\cos^2\theta + 1)}\,S_{11} + \overline{\cos^2\theta}\,S_{12} + \tfrac{1}{4}\overline{(\sin^2\theta\cos^2\theta + 3\cos^2\theta)}\,S_{13} + \tfrac{1}{8}\overline{\sin^4\theta}\,S_{33} + \tfrac{1}{8}\overline{(\sin^2\theta\cos^2\theta - \sin^2\theta)}\,S_{44}$$

$$\bar{S}'_{13} = \tfrac{1}{2}\overline{\sin^2\theta\cos^2\theta}\,S_{11} + \tfrac{1}{2}\overline{\sin^2\theta}\,S_{12} + \tfrac{1}{2}\overline{(\sin^4\theta + \cos^4\theta + \cos^2\theta)}\,S_{13} + \tfrac{1}{2}\overline{\sin^2\theta\cos^2\theta}\,S_{33} - \tfrac{1}{2}\overline{\sin^2\theta\cos^2\theta}\,S_{44}$$

where a prime denotes the compliance for the aggregate and the umprimed compliances are those of the transversely isotropic unit.

3. Experiment

3.1. The Fibre Samples and their Preparation

The five materials used in the present investigation were: low density (branched) polyethylene ("Alkathene", ICI Ltd), high density (linear) polyethylene ("Rigidex", British Hydrocarbon Chemicals); polyethylene terephthalate ("Terylene", ICI Ltd); nylon 6.6 ("Luron", ICI Ltd) and polypropylene (from "Propathene" polymer, ICI Ltd). All fibres contained small quantities of additives, as used in commercial materials, but in insufficient quantities to affect the overall characteristics of the polymer.

All samples were in the form of monofilaments obtained by a conventional two-stage melt spinning and drawing process. Molten polymer was extruded under pressure and wound on a bobbin, conditions being chosen so that the resulting spun filaments had a very low degree of orientation. These filaments were subsequently drawn (i.e., stretched) to varying degrees of molecular alignment. The drawing process was normally continuous, with the filament being stretched in a heated zone between two sets of rolls moving at different speeds, the draw-ratio being governed by the relative speed of the rolls. True draw-ratio was determined by comparing filament diameters before and after stretching. For the case of low density polyethylene drawing was carried out by stretching filaments mounted in an Instron tensile testing machine. The drawn monofilaments typically had diameters in the range 0.01 to 0.03 cm, a diameter small enough to yield a circular cross-section yet large enough to simplify experimental measurements.

Optical anisotropy (birefringence) was measured using a polarising microscope fitted with a Berek compensator; inspection under an interference microscope determined whether the filaments were of uniform composition.

In certain cases newly-drawn fibres, or those remaining wound on a bobbin for any length of time, were in a non-equilibrium state, and their mechanical properties depended on the time between sample preparation and testing. All samples were thus permitted to relax before testing for sufficient time for reproducibility to be attained.

The properties of the nylon filaments were sensitive to humidity; all tests on these samples were therefore carried out under controlled conditions. All other tests were carried out in an open laboratory at a temperature of 21 $\pm$ 2° C.

3.2. Experimental Principles and Procedure

3.2.1. Extensional Measurements

The extensional compliances of the monofilaments (S'_{33}) were determined by measuring their extensions under a range of loads, using a travelling microscope. Measurements were recorded 1 min after loading, 10 min recovery then being allowed before a further load was added. Slight non-linearity (i.e. strain-dependence of compliance) was shown, particularly with polypropylene, and so all results are quoted at strains of 0.005. To ensure reproducibility all filaments were subjected to an initial mechanical conditioning treatment, in which the maximum load was applied and removed several times, using the standard 1 min on, 10 min off, cycle [8].

3.2.2. Axial Poisson's Ratio

The axial Poisson's ratio ($\nu_E = -S'_{13}/S'_{33}$) was measured directly from the change in diameter of a monofilament which was extended between the two movable clamps of a specially constructed microscope stage; two ink marks on the filament acted as reference points for measurements of length and changes of length [9]. All measurements were made with the aid of a calibrated eyepiece. An immersion liquid was used to reduce diffraction effects at the edges of the filament.

3.2.3. Transverse Compression

Hertzian contact theory has been extended to account for the compression of a monofilament (a transversely isotropic cylinder) between parallel rigid flats. The quantities which have

been measured are the contact width between cylinder and plates ($2b$), and the change in diameter parallel to the plane of contact (U_1). It has been shown elsewhere [8, 9] that

$$b^2 = \frac{4FR}{\pi} [S'_{11} - \nu_E^2 S'_{33}]$$

$$U_1 = F \left[\left(\frac{4}{\pi} - 1 \right) (S'_{11} - \nu_E^2 S'_{33}) - (S'_{12} - \nu_E^2 S'_{33}) \right]$$

where R is the radius of the filament and F the load per unit length of contact.

Textile filaments are much stiffer along their axis than transverse to it, and S'_{33} therefore is appreciably smaller than S'_{11}. Since Poisson's ratio is unlikely to be much different from 0.5, it follows that the second term is only a small correction factor, with the contact width depending primarily on S'_{11}.

The diameter change U_1 depends primarily on S'_{12}, although there is a substantial term of approximately 0.25 S'_{11}. Again the quantity $\nu_E^2 S'_{33}$ will be only a small correction term.

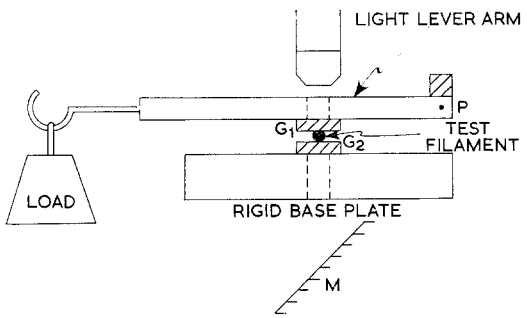

Figure 1 Schematic side elevation of fibre compression apparatus (not to scale). Key: G_1, G_2, glass blocks; P, adjustable pivot; M, mirror.

Measurements were performed using the apparatus shown schematically in fig. 1. The monofilament was compressed between the two parallel glass blocks G_1 and G_2 and the contact width was measured from a projected image of the contact zone seen in reflected light. Surface roughness and asperities were evident only at the lowest loads. The interference fringes visible on either side of the contact zone could be used to extrapolate to the true contact width, but the correction was small compared with experimental error.

Changes in transverse diameter U_1 were measured directly, using a calibrated eyepiece. In this case the filament was surrounded by a suitable immersion liquid.

3.2.4. Torsion Measurements

The torsional modulus was measured using a free vibration torsion pendulum of the design described by Meredith [10]. The modulus was calculated from the period of oscillation by applying the standard formula for a cylindrical rod.

3.3. Experimental Accuracy

Viscoelastic effects, accuracy of instrumental readings and in the case of nylon the relative humidity, all affect the accuracy of measurements on a particular fibre. The major source of error was, however, the wide variation between nominally identical samples. This variation was smallest for measurements of extensional compliance, where the value measured was an average over a 60 cm length, and largest for Poisson's ratio measurements which involved changes in filament diameter over a mean sample length of less than 0.1 cm. A standard error of only 5% on the mean value of extensional compliance was frequently obtained from measurements on five to ten samples, whilst S'_{12} and S'_{13} could show standard errors of 30 to 40% for a similar number of samples.

The variability in torsional and transverse compliance experiments, where the sample lengths were several cm and several mm respectively, was intermediate between the limits above. Since these experiments were relatively simple to perform the number of samples measured could be increased to yield an overall accuracy comparable with that for the extensional measurements.

4. Results

Fig. 2 shows the extensional modulus ($1/S'_{33}$) of polyethylene terephthalate (PET) measured as a function of both optical birefringence and draw-ratio; also shown is the relation between draw-ratio and birefringence. In some samples of PET the skin of the fibre was not identical with the core, and showed a different relationship between birefringence and draw-ratio [11]. Similar relationships for the other polymers tested are shown in fig. 3; no differential skin/core effect was observed in these materials.

Figs. 4-8 compare the measured variations of extensional modulus ($1/S'_{33}$), transverse modulus

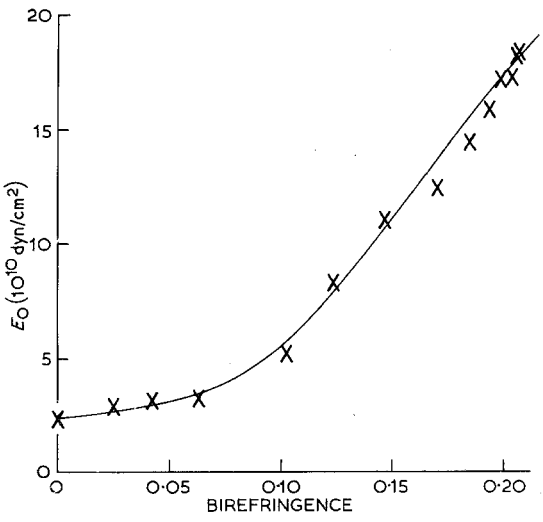

(a)

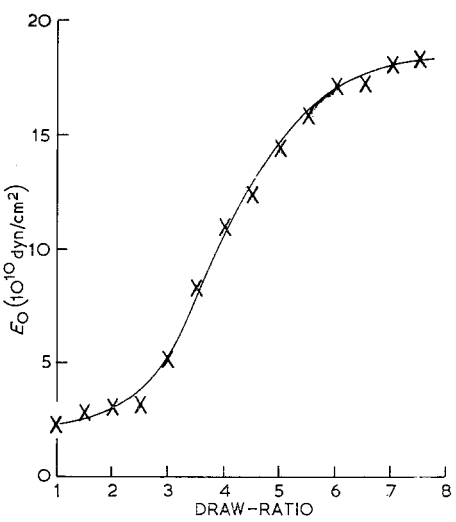

(b)

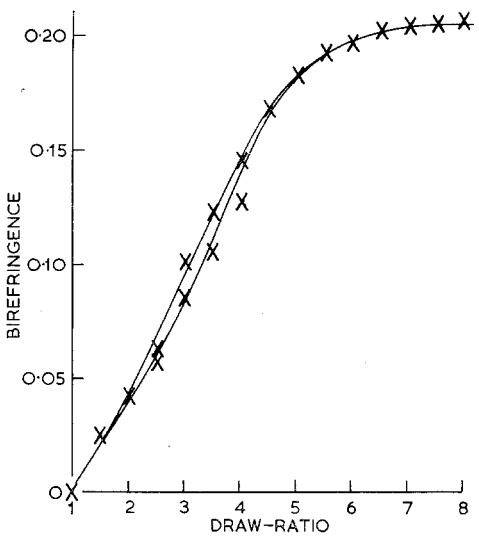

(c)

Figure 2 Polyethylene terephthalate fibres: variation of extensional modulus with birefringence (a) and draw-ratio (b) together with relation between birefringence and draw-ratio (c).

$(1/S'_{11})$ and torsional modulus $(1/S'_{44})$, all plotted as functions of draw-ratio, with predicted Reuss and Voigt average values. These theoretical values were calculated initially on the assumption that the elastic constants for the most highly-oriented fibres measured were those appropriate to the fully-oriented filaments. In certain cases the fit could be improved somewhat by extrapolating from measured values to estimate the compliances for a fibre of maximum calculated birefringence. (Moduli rather than compliances have been plotted to reduce the data to more conventional forms.)

Fig. 9 shows the effect of relative humidity on the extensional and torsional moduli of nylon,

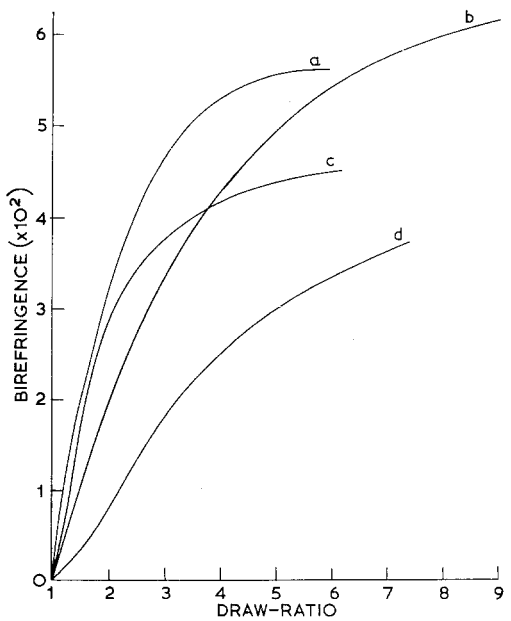

Figure 3 Relation between birefringence and draw-ratio for fibres of (a) nylon, (b) high-density polyethylene, (c) low-density polyethylene (d) polypropylene.

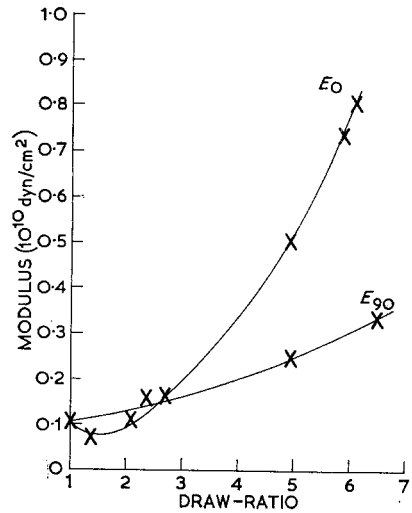

(a)

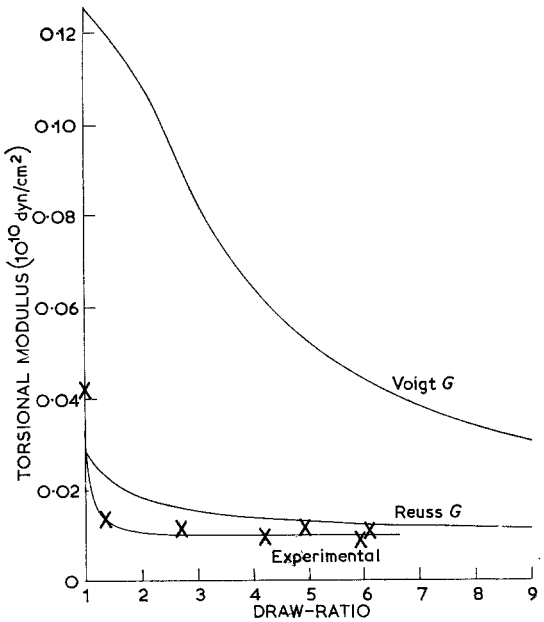

(b)

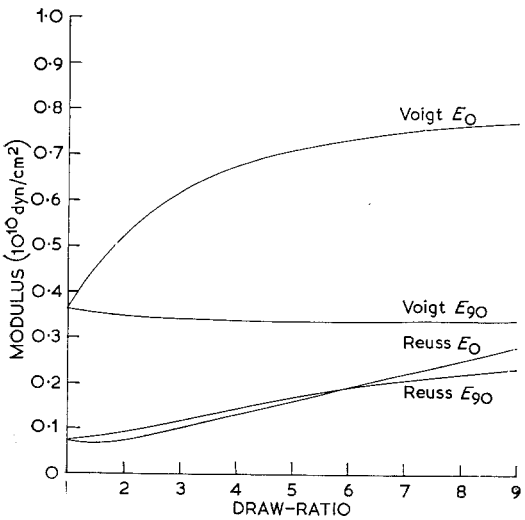

(c)

Figure 4 Low density polyethylene: extensional (E_0), transverse (E_{90}) and torsional moduli (G), comparison between experimental results and simple aggregate theory for E_0 and E_{90} (a) and (c), and for G (b).

and illustrates the necessity for keeping humidity constant. In subsequent work (fig. 8) the relative humidity was controlled at 20%, in a region where there is minimum sensitivity to small changes about the mean value.

Measurements of all five elastic compliances at selected degrees of orientation are shown in table I, which contains also the results of Raumann [12, 13] for low density polyethylene film. Values of S'_{33}, S'_{11} and S'_{44} for highly oriented and unoriented (macroscopically isotropic) filaments are given in table II. For the latter samples $S'_{11} = S'_{33}$. Finally, in table III, comparisons are made between the measured values of S'_{33} and S'_{44} and the values calculated from the aggregate theory using both Reuss and Voigt approximations.

5. Discussion

5.1. General Features of Birefringence

In general terms the birefringence/draw-ratio curves all take a similar form, as noted previously by several writers (e.g. Crawford and Kolsky for polyethylene [14], Cannon and Chappel for nylon [15], with the birefringence increasing rapidly at low draw-ratios, but approaching the maximum value asymptotically at draw-ratios greater than about five. Crawford and Kolsky concluded that the birefringence was directly related to the permanent strain, and they proposed a model of rod-like crystallites in a matrix, the symmetry axes of the crystallites rotating towards the draw direction on drawing. This model was later generalised to an aggregate of transversely isotropic units of known optical and mechanical anisotropy [5], and used to describe

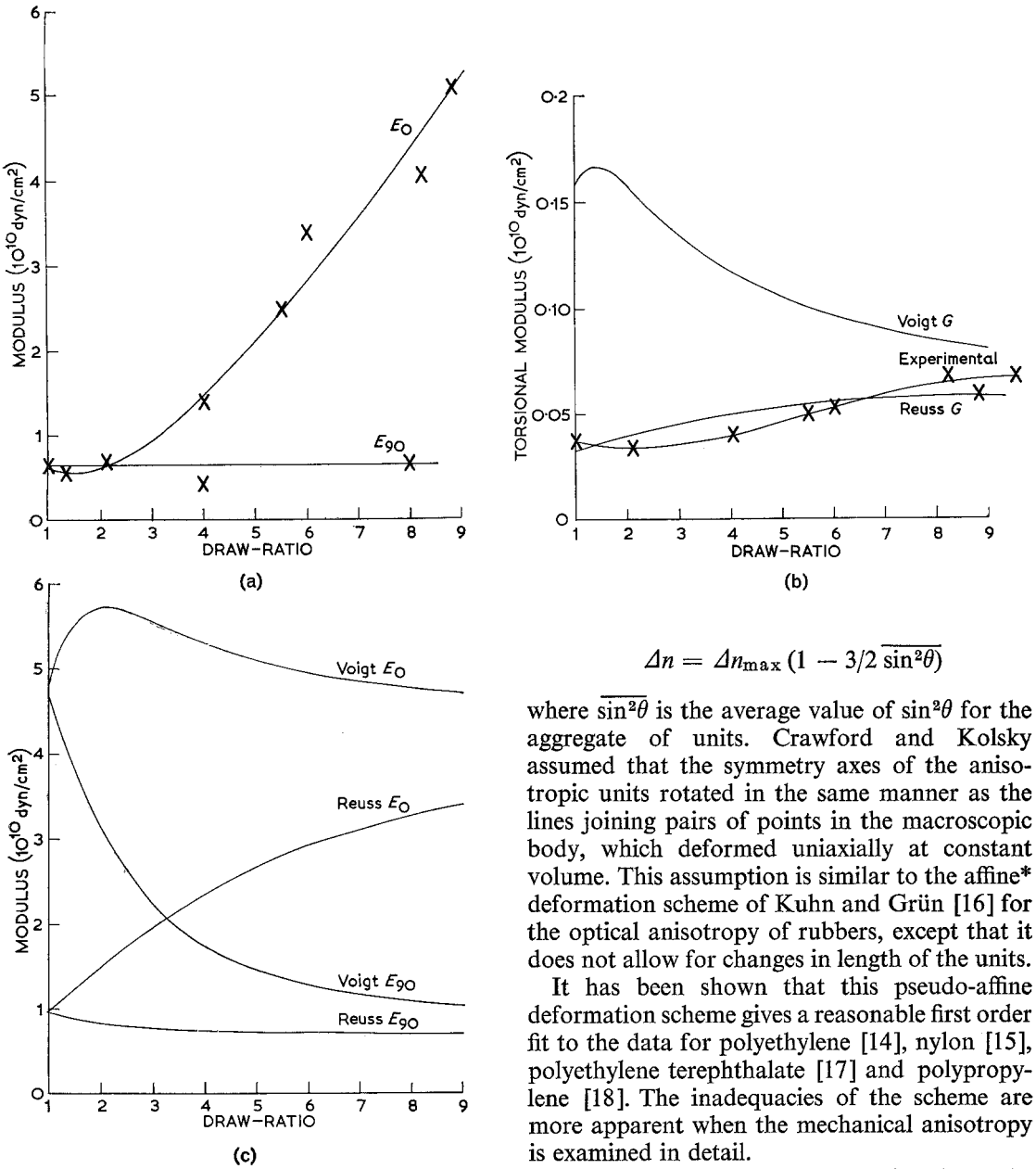

Figure 5 High density polyethylene filaments: extensional (E_o), transverse (E_{90}) and torsional moduli (G) comparison between experimental results and simple aggregate theory for E_o and E_{90} (a) and (c), and for G (b).

optical and mechanical data on oriented sheets of low density polyethylene.

On this model the birefringence Δn of a fibre is given by

$$\Delta n = \Delta n_{\max}(1 - 3/2\,\overline{\sin^2\theta})$$

where $\overline{\sin^2\theta}$ is the average value of $\sin^2\theta$ for the aggregate of units. Crawford and Kolsky assumed that the symmetry axes of the anisotropic units rotated in the same manner as the lines joining pairs of points in the macroscopic body, which deformed uniaxially at constant volume. This assumption is similar to the affine* deformation scheme of Kuhn and Grün [16] for the optical anisotropy of rubbers, except that it does not allow for changes in length of the units.

It has been shown that this pseudo-affine deformation scheme gives a reasonable first order fit to the data for polyethylene [14], nylon [15], polyethylene terephthalate [17] and polypropylene [18]. The inadequacies of the scheme are more apparent when the mechanical anisotropy is examined in detail.

For the hot-drawn fibres studied here the pseudo-affine deformation scheme predicts orientations at low draw-ratios which are greater than those found experimentally, and the converse situation at high draw-ratios. In polyethylene terephthalate, where the maximum birefringence can be predicted with some confidence from bond polarisabilities (Pinnock and Ward [11], quoting Mr R. P. Palmer's data), it was found that empirically the birefringence was related to a

*In the affine deformation scheme of Kuhn and Grün the cross-link points of the rubber network can be considered to deform in an identical manner to points marked in the macroscopic body.

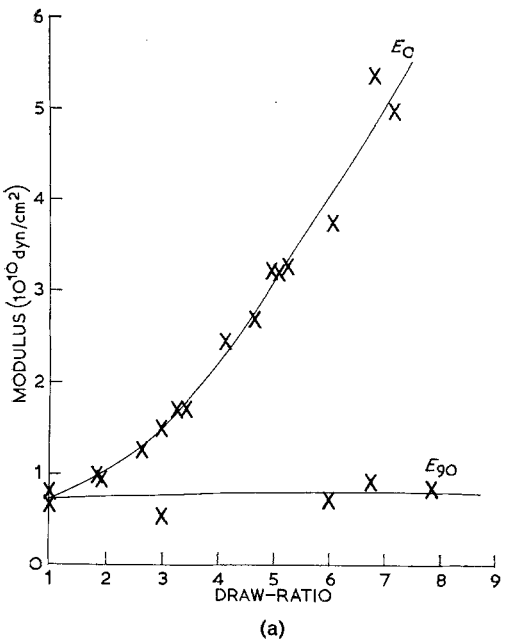

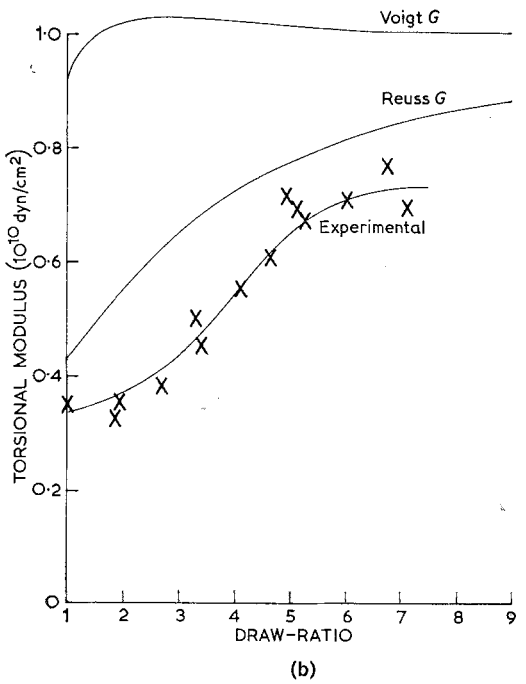

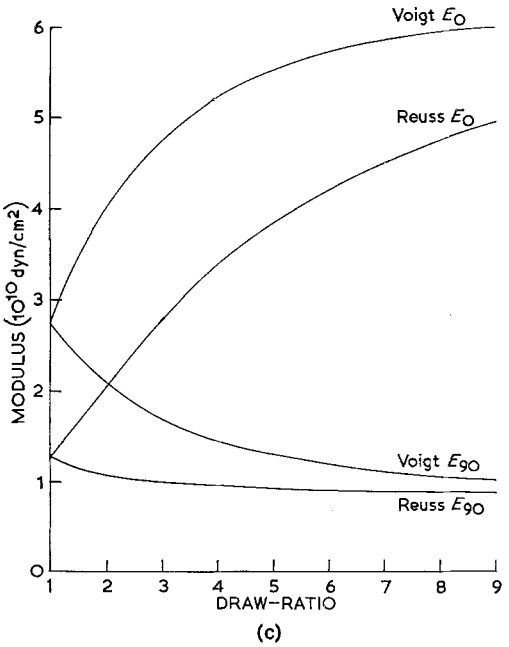

Figure 6 Polypropylene filaments: extensional (E_0), transverse (E_{90}) and torsional moduli (G); comparison between experimental results and simple aggregate theory for E_0 and E_{90} (a) and (c), and for G (b).

logarithmic function of draw-ratio. In cold-drawn polyethelene terephthalate fibres, on the other hand, an exact fit with the predictions of the pseudo-affine deformation scheme was obtained [17], showing that the exact nature of the drawing process is important in determining the distribution of molecular orientations.

In both polyethylene and polypropylene there is considerable difficulty in obtaining an accurate estimate of the maximum birefringence since the necessary assumption of additivity of bond polarisabilities seems likely not to hold for the C—C bond [19]. In polypropylene, where a detailed study has been carried out [18], it was concluded that the divergence between measured and predicted birefringence was similar to that observed in polyethylene terephthalate.

It can be concluded therefore, on the evidence of birefringence data, that the pseudo-affine deformation scheme applies even as a first approximation only to the hot-drawing of polymers.

5.2. General Features of Mechanical Anisotropy

The exact development of mechanical anisotropy with draw-ratio will depend on details both of the

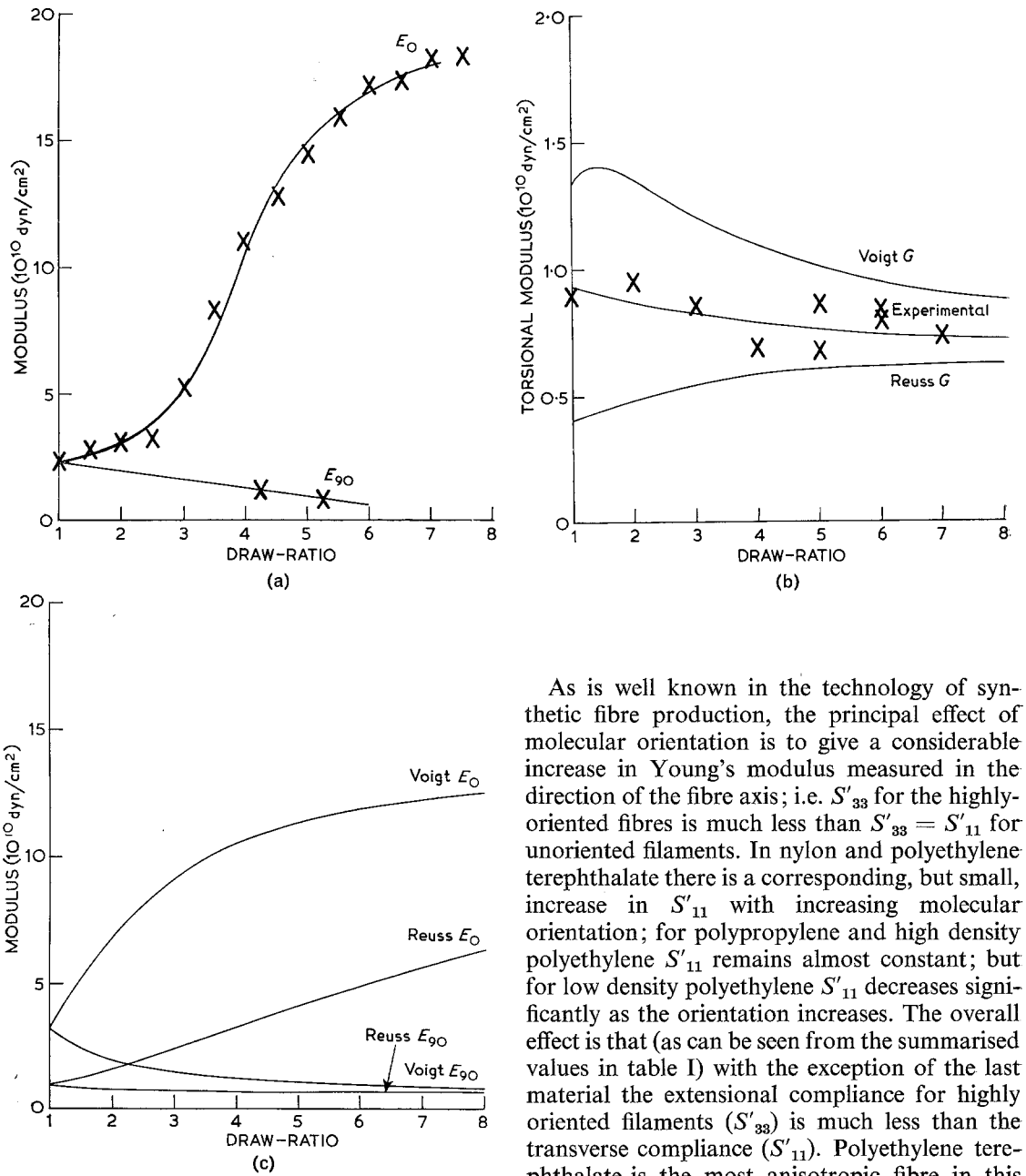

Figure 7 Polyethylene terephthalate filaments: extensional (E_o), transverse (E_{90}) and torsional moduli (G); comparison between experimental results and simple aggregate theory for E_o and E_{90} (a) and (c), and for G (b).

composition of the fibres and of the drawing process. However, the examination of the arbitrary set of commercially-produced fibres discussed here shows general features characteristic of each polymer.

As is well known in the technology of synthetic fibre production, the principal effect of molecular orientation is to give a considerable increase in Young's modulus measured in the direction of the fibre axis; i.e. S'_{33} for the highly-oriented fibres is much less than $S'_{33} = S'_{11}$ for unoriented filaments. In nylon and polyethylene terephthalate there is a corresponding, but small, increase in S'_{11} with increasing molecular orientation; for polypropylene and high density polyethylene S'_{11} remains almost constant; but for low density polyethylene S'_{11} decreases significantly as the orientation increases. The overall effect is that (as can be seen from the summarised values in table I) with the exception of the last material the extensional compliance for highly oriented filaments (S'_{33}) is much less than the transverse compliance (S'_{11}). Polyethylene terephthalate is the most anisotropic fibre in this respect, with $S'_{11}/S'_{33} \sim 27$. Note the anomalous behaviour of low density polyethylene at draw-ratios less than 2. In this region $S'_{11} < S'_{33}$, with S'_{33} showing a relatively large maximum at low draw-ratios and S'_{33} only a shallow maximum. These features have been discussed in detail elsewhere [13, 20].

A further striking difference between low density polyethelene and the other fibres was shown by the change of the shear modulus

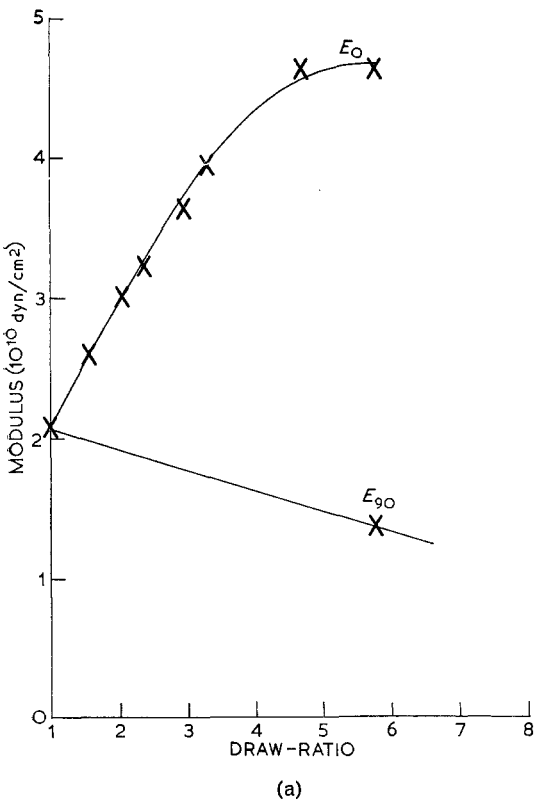

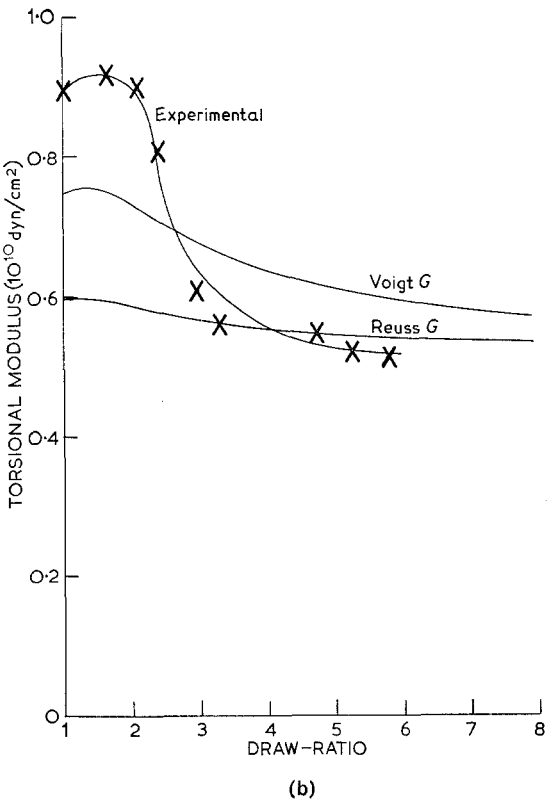

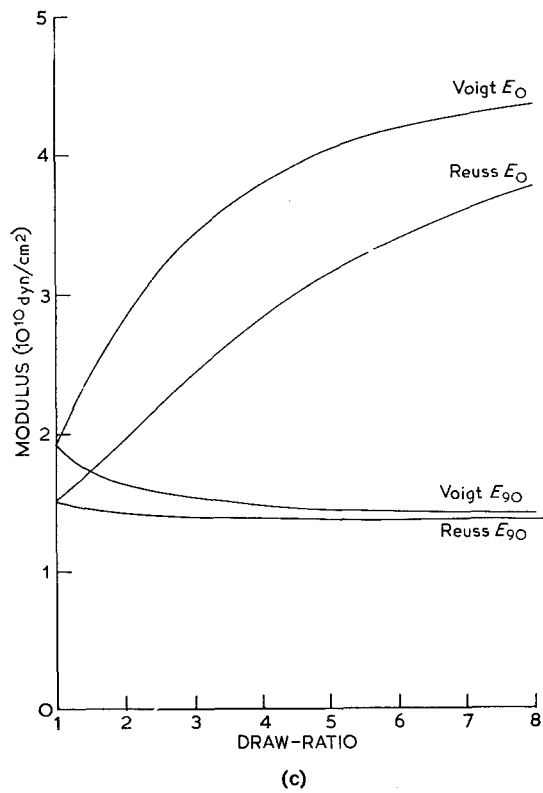

Figure 8 Nylon filaments: extensional (E_0), transverse (E_{90}) and torsional moduli (G); comparison between experimental results and simple aggregate theory for E_0 and E_{90} (a) and (c), and for G (b).

$(1/S'_{44})$ on orientation, a decrease greater than three times occurring over the range of orientations examined, compared with only small changes for the other materials. For these other fibres S'_{44} lay close in value to S'_{11}: in polyethylene terephthalate, high density polyethylene and polypropylene $S'_{44}/S'_{11} \sim 1$: in nylon $S'_{44}/S'_{11} \sim 2$. Low density polyethylene appears, as far as the present room temperature measurements are concerned, to be an exceptional polymer in all respects, with the extensional compliance having the same order of magnitude as the transverse compliance, and the shear compliance (S'_{44}) being more than an order of magnitude greater than either S'_{33} or S'_{11}. This exceptional behaviour was borne out by subsequent detailed analysis, which is the subject of a series of separate publications [20, 21].

It is interesting to note the similarity between the elastic constants of high density polyethylene and polypropylene: the relative values of the

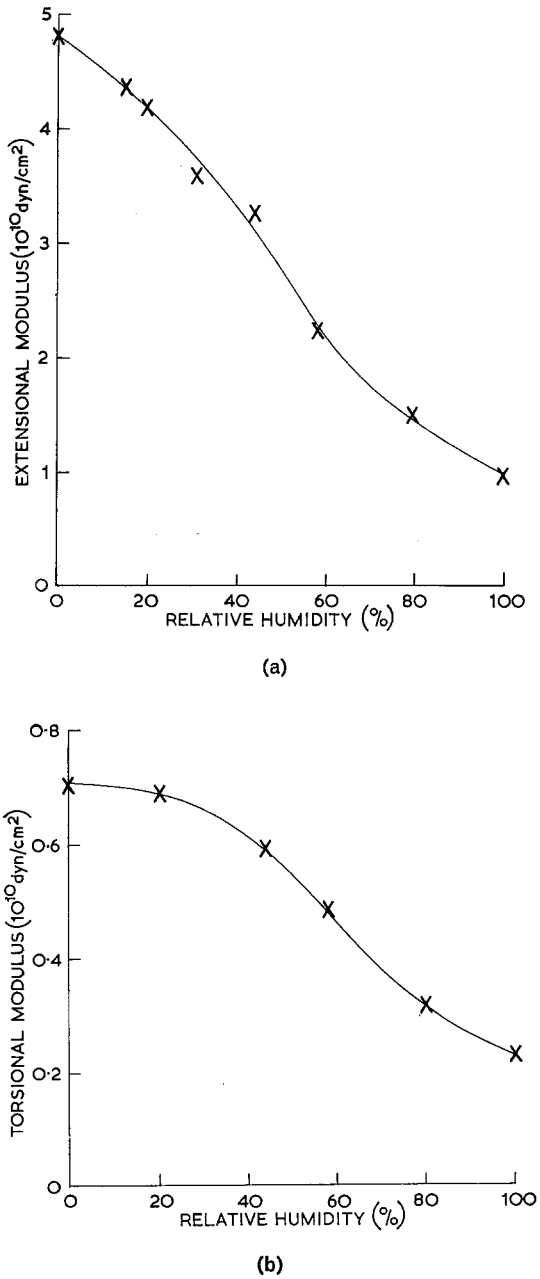

Figure 9 Highly-drawn nylon filament: effect of relative humidity at 21° C on extensional (a) and torsional moduli (b).

elastic compliances show very similar trends, and the major differences can be expressed by the greater stiffness of polypropylene, as might be expected from its higher melting point.

The compliance $-S'_{13}$ was in all cases low, and appeared (within the range of data obtained) to decrease rapidly with increasing draw-ratio, in a parallel manner to S'_{33}. Thus Poisson's ratio ($\nu_E = -S'_{13}/S'_{33}$) was rather insensitive to draw-ratio and, with the exception of highly oriented high density polyethylene, did not differ significantly from 0.50. The assumption that the fibres are incompressible is thus generally a valid approximation. (Note that for anisotropic bodies ν_E is not confined to values < 0.50, but is limited solely by the inequalities necessary for a positive strain energy: $S'^2_{12} < S'_{11}S'_{13}$; $S'^2_{13} < \frac{1}{2}S'_{33}(S'_{11} + S'_{12})$, see for example Nye [4].)

The "transverse Poisson's ratio" ($\nu_T' = -S'_{12}/S'_{11}$) was subject to large experimental errors, but even so the values can be seen to range widely, with those for polypropylene and high density polyethylene being considerably higher than for the other three materials.

Two small unusual features of the mechanical anisotropy of the fibres examined have not previously been reported. There is a small minimum in the extensional modulus of high density polyethylene at low draw-ratios, and a very small maximum in the torsional modulus of nylon at a draw-ratio of 1.5.

5.3. Correlation of the Elastic Compliances between Oriented and Unoriented Fibres

Investigations of the relationships between mechanical anisotropy and structure of oriented polymers [15, 11, 18, 20, 21] have shown that, although the morphological structure can be important in some details, the molecular orientation is usually the primary factor in determining the mechanical anisotropy. It has been found useful in the analysis of the anisotropy to consider that the unoriented or partially oriented polymer or fibre can be regarded, as explained in section 2.2, as an aggregate of anisotropic elastic units whose properties are those of the perfectly oriented material. Different values for the elastic constants of the aggregate are predicted by the Reuss (constant stress) and Voigt (constant strain) approximations. It has been shown by Bishop and Hill [22], on energy considerations, that the correct value for a random aggregate lies between the extreme values predicted by the alternative schemes above.

In table III the measured compliances for unoriented fibres are compared with those calculated on the basis of the Reuss and Voigt averaging procedures. For the cases of polyethylene terephthalate and low density polyethylene the

TABLE I Elastic compliances of oriented fibres (units of compliance are $cm^2/dyn \times 10^{-11}$; errors quoted are 95% confidence limits).

Material	Birefringence ($\triangle n$)	S'_{11}	S'_{12}	S'_{33}	S'_{13}	S'_{44}	$E = -\frac{S'_{13}}{S'_{33}}$	$E' = -\frac{S'_{12}}{S'_{11}}$
Low density polyethylene film (Raumann [14])	—	22	− 15	14	− 7	680	0.50	0.68
Low density polyethylene 1	0.0361	40± 4	− 25± 4	20± 2	− 11± 2	878± 56	0.55± 0.08	0.61± 0.20
Low density polyethylene 2	0.0438	30± 3	− 22± 3	12± 1	− 7± 1	917± 150	0.58± 0.08	0.73± 0.20
High density polyethylene 1	0.0464	24± 2	− 12± 1	11± 1	− 5.1± 0.7	34± 1	0.46± 0.15	0.52± 0.08
High density polyethylene 2	0.0594	15± 1	− 16± 2	2.3± 0.3	− 0.77± 0.3	17± 2	0.33± 0.12	1.1± 0.14
Polypropylene 1	0.0220	19± 1	− 13± 2	6.7± 0.3	− 2.8± 1.0	18± 1.5	0.42± 0.16	0.68± 0.18
Polypropylene 2	0.0352	12± 2	− 17± 2	1.6± 0.04	− 0.73± 0.3	10± 2	0.47± 0.17	1.5± 0.3
Polyethylene terephthalate 1	0.153	8.9± 0.8	− 3.9± 0.7	1.1± 0.1	− 0.47± 0.05	14± 0.5	0.43± 0.06	0.44± 0.09
Polyethylene terephthalate 2	0.187	16± 2	− 5.8± 0.7	0.71± 0.04	− 0.31± 0.03	14± 0.2	0.44± 0.07	0.37± 0.06
Nylon	0.057	7.3± 0.7	− 1.9± 0.4	2.4± 0.3	− 1.1± 0.15	15± 1	0.48± 0.05	0.26± 0.08

TABLE II Comparison of elastic compliances of highly-oriented and unoriented fibres (units of compliance are $cm^2/dyn \times 10^{-11}$).

	Highly-oriented			Unoriented	
	S'_{11}	S'_{33}	S'_{44}	$S'_{11}=S'_{33}$	S'_{44}
Low density polyethylene	30	12	917	81	238
High density polyethylene	15	2.3	17	17	26
Polypropylene	12	1.6	10	14	27
Polythylene terephthalate	16	0.71	14	4.4	11
Nylon	7.3	2.4	15	4.8	12

measured isotropic compliances lie between the calculated bounds, suggesting that in these polymers the molecular orientation is indeed the primary factor determining the mechanical anisotropy. In nylon the measured compliances lie just outside the bounds, suggesting that although molecular orientation is important in determining the mechanical anisotropy, other factors also play an important part. Finally, in high density polyethylene and polypropylene the measured values for the isotropic compliance $S'_{11} = S'_{33}$ lie well outside the calculated bounds, suggesting that factors other than orientation play a major role in the mechanical behaviour.

5.4. Theoretical Attempts to Predict the Mechanical Anisotropy

The elastic constants of a partially oriented polymer can be predicted without obtaining the distribution of orientation of the units. It is

TABLE III Comparison of calculated and measured extensional and torsional compliances for unoriented fibres (units are $cm^2/dyn \times 10^{11}$).

	Extensional compliance ($S'_{11}=S'_{33}$)			Torsional compliance (S'_{44})		
	Calculated		Measured	Calculated		Measured
	Reuss av	Voigt av		Reuss av	Voigt av	
Low density polyethylene	139	26	81	416	80	238
High density polyethylene	10	2.1	17	30	6	26
Polypropylene	7.7	3.8	14	23	11	2.7
Polyethylene terephthalate	10.4	3.0	4.4	25	7.6	111
Nylon	6.6	5.2	4.8	17	13	12

necessary, as discussed in detail elsewhere [5, 24], only to use the spherical harmonic functions P_2 and P_4 relating to $\overline{\cos^2\theta}$ and $\overline{\cos^4\theta}$, where θ is the angle between the axis of an elastic unit in the aggregate and the fibre axis. Only in the case of low density polyethylene have attempts been made by X-ray and nuclear magnetic resonance methods to determine these spherical harmonic functions by direct measures [23, 24].

It can be seen from figs. 4-8 that the aggregate model incorporating the pseudo-affine deformation scheme can predict the general form of the mechanical anisotropy. As reported previously [5] the predicted Reuss average curves for low density polyethylene (the only set obtainable at the time since S'_{12} had not then been measured) show the correct overall pattern, including the minimum in the extensional modulus. This feature arises because of the extremely large shear compliance S'_{44} for the highly-oriented fibre (the unit of the model) compared with S'_{11} and S'_{33}, which are approximately equal. Recent work [20, 25] attempts to relate the high shear compliance to structural features; *viz* a molecular motion parallel to the molecular chains in the crystallites.

The theoretical curves differ from those obtained experimentally in two ways. First there are features of detail (a small minimum in the transverse modulus for low density polyethylene; a small minimum in the extensional modulus for high density polyethylene) which are not predicted at all. It will be shown elsewhere [26] that such effects can be associated with mechanical twinning. Secondly the predicted development of mechanical anisotropy with increasing draw-ratio is much less rapid than is observed in practice. Deficiencies in the pseudo-affine deformation scheme are not unexpected because of the simplifying nature of the assumptions made. In low density polyethylene a considerably improved fit was obtained by taking the measured orientation functions [23, 24].

The aggregate model predicts only that the elastic constants should lie between the Reuss and Voigt average values. In polyethylene terephthalate it is clear that experimental compliances lie approximately midway between the two bounds. For cold-drawn fibres this median condition applies almost exactly [17].

For low density polyethylene, however, a Voigt averaging scheme does not predict the anomalous behaviour; thus the Reuss average appears to describe the physical situation more closely. A similar conclusion was reached by Odajima and Maeda [27], who compared theoretical estimates of the Reuss and Voigt averages of single crystals of polyethylene with experimental values.

In nylon it would appear that the Voigt average is closest to the experimentally observed data. It is interesting to note that both averaging schemes predict a maximum in the torsional modulus as a function of draw-ratio.

The aggregate model would not appear to be generally applicable to high density polyethylene and polypropylene. Pinnock and Ward [18] had earlier concluded that for polypropylene the aggregate model was applicable only at low draw-ratios. It would appear that for high draw-ratios, quite apart from the degree of orientation, simultaneous changes occur in morphology and molecular mobility, both of which affect the mechanical properties.

All the experimental work was performed at room temperature. It has since been shown [20] that the anomalous behaviour of low density polyethylene film at low draw-ratios disappears at sufficiently low temperatures, and it is thus feasible that for all polymers the applicability of either the Reuss or Voigt type schemes might be dependent on the temperature at which the investigations were carried out.

6. Conclusions

The aggregate model meets with some success in attempting to predict the mechanical anisotropy of oriented polymeric fibres. In its simplified form where pseudo-affine deformation is assumed, the Reuss average can predict to a first approximation the overall patterns of mechanical anisotropy. With direct measurement of the required orientation functions the theory can in some cases give a quantitative fit to the experimental data. It appears that in low density polyethylene the Reuss average describes the physical situation more closely than the Voigt average; in nylon the Voigt average appears to be more applicable; and in polyethylene terephthalate the measured values are close to the mean of the two averages. It is considered that these conclusions will relate to the detailed nature of the stress and strain distributions at a molecular level in the fibres, and should in turn be related to the structure.

In two fibres, high density polyethylene and polypropylene, the aggregate model appears at this stage to be of very limited applicability,

probably because of complex changes in morphology and molecular mobility which occur on drawing.

References

1. I. M. WARD, *Appl. Mat. Res.* **5** (1966) 224.
2. I. M. WARD and P. R. PINNOCK, *Brit. J. Appl. Phys.* **17** (1966) 3.
3. R. F. S. HEARMON, *Adv. Phys.* **5** (1956) 323.
4. J. F. NYE, "Physical Properties of Crystals" (Clarendon Press, Oxford, 1957).
5. I. M. WARD, *Proc. Phys. Soc.* **80** (1962) 1176.
6. A. REUSS, *Z. Angew. Math. Mech* **9** (1929) 49.
7. W. VOIGT, Lehrbuch der Kristallphysik (Teubner, Leipzig, 1928) p. 410.
8. D. W. HADLEY, I. M. WARD, and J. WARD, *Proc. Roy. Soc.* **A285** (1965) 275.
9. P. R. PINNOCK, I. M. WARD, and J. M. WOLFE, *ibid* **A291** (1966) 267.
10. R. MEREDITH, *J. Text. Inst.* **45** (1954) T489.
11. P. R. PINNOCK and I. M. WARD, *Brit. J. Appl. Phys.* **15** (1964) 1559.
12. G. RAUMANN and D. W. SAUNDERS, *Proc. Phys. Soc.* **77** (1961) 1028.
13. G. RAUMANN, *ibid* **79** (1962) 1221.
14. S. M. CRAWFORD and H. KOLSKY, *ibid* **B64** (1951) 119.
15. C. G. CANNON and F. P. CHAPPEL, *Brit. J. Appl. Phys* **10** (1959) 68.
16. W. KUHN and F. GRÜN, *Kolloid-Z.* **101** (1942) 248.
17. S. W. ALLISON and I. M. WARD, *Brit. J. Appl. Phys.* **18** (1967) 1151.
18. P. R. PINNOCK and I. M. WARD, *ibid* **17** (1966) 575.
19. D. A. KEEDY, J. POWERS, and R. S. STEIN, *J. Appl. Phys.* **31** (1960) 1911.
20. V. B. GUPTA and I. M. WARD, *J. Macromol. Sci. (Phys.)* **B(i)2** (1967) 373.
21. *Idem, ibid* **B(ii)1** (1968) 89.
22. J. BISHOP and R. HILL, *Phil. Mag.* **42** (1951) 414; 1298.
23. V. B. GUPTA, A. KELLER, and I. M. WARD, *J. Macromol. Sci. (Phys.)* **B(ii)1** (1968) 139.
24. V. J. MCBRIERTY and I. M. WARD, *Brit. J. Appl. Phys.* **ser 2,1** (1968) 1529.
25. Z. H. STACHURSKI and I. M. WARD, *J. Polymer. Sci.* **A26** (1968) 1083.
26. F. C. FRANK, V. B. GUPTA, and I. M. WARD, unpublished work.
27. A. ODAJIMA and I. MAEDA, *Report Prog. Polymer Phys. Japan* **9** (1966) 169.